Dominant effects of an Msh6 missense mutation on DNA repair and cancer susceptibility

Guohze Yang,[1,6] Stefan J. Scherer,[1,6] Scarlet S. Shell,[3] Kan Yang,[4] Mimi Kim,[2] Martin Lipkin,[4] Raju Kucherlapati,[5] Richard D. Kolodner,[3,*] and Winfried Edelmann[1,*]

[1]Department of Cell Biology
[2]Department of Epidemiology and Population Health
Albert Einstein College of Medicine, Bronx, New York 10461
[3]Ludwig Institute for Cancer Research, Cancer Center and Department of Medicine, University of California San Diego, La Jolla, California 92093
[4]Strang Cancer Center at The Rockefeller University, New York, New York 10021
[5]Harvard-Partners Center for Genetics and Genomics, Harvard Medical School, Boston, Massachusetts 02115
[6]These authors contributed equally to this work.
*Correspondence rkolodner@ucsd.edu, edelmann@aecom.yu.edu

Summary

Mutations in DNA mismatch repair (MMR) genes cause hereditary nonpolyposis colorectal cancer (HNPCC), and MMR defects are associated with a significant proportion of sporadic cancers. MMR maintains genome stability and suppresses tumor formation by preventing the accumulation of mutations and by mediating an apoptotic response to DNA damage. We describe the analysis of a dominant *MSH6* missense mutation in yeast and mice that causes loss of DNA repair function while having no effect on the apoptotic response to DNA damaging agents. Our results demonstrate that *MSH6* missense mutations can effectively separate the two functions, and that increased mutation rates associated with the loss of DNA repair are sufficient to drive tumorigenesis in MMR-defective tumors.

Introduction

DNA mismatch repair (MMR) functions to repair misincorporation errors that occur during DNA replication and acts on mispaired bases formed in recombination intermediates (Buermeyer et al., 1999; Kolodner, 1996; Kolodner and Marsischky, 1999; Modrich and Lahue, 1996). As a consequence of the role of MMR in DNA replication, MMR-defective cells have high mutation rates. MMR acts to prevent recombination between divergent DNA sequences, and as a consequence, MMR may also act to prevent some types of genome rearrangements (Evans and Alani, 2000; Harfe and Jinks-Robertson, 2000; Myung et al., 2001). MMR proteins also play a role in some cellular responses to DNA damage, and consequently, MMR-defective mammalian cells are resistant to killing by DNA-damaging agents, including some types of chemotherapeutic agents (Aebi et al., 1996; Bignami et al., 2003; D'Atri et al., 1998; Li, 1999; Modrich, 1997). MMR defects can underlie the development of cancer. HNPCC is an inherited cancer susceptibility syndrome where, in many cases, the tumors show microsatellite instability (MSI) indicative of a MMR defect (Peltomaki, 2003). The majority of these HNPCC cases are due to inherited mutations in two MMR genes, *MSH2* and *MLH1* (Peltomaki, 2003; Yan et al., 2000). A small number of HNPCC cases are due to inherited mutations in *MSH6*, whereas a larger number of later onset familial atypical-HNPCC cases are due to mutations in *MSH6* (Akiyama et al., 1997; Berends et al., 2002; Kolodner et al., 1999; Miyaki et al., 1997). Sporadic MMR-defective cancers are largely due to somatic silencing of the *MLH1* gene (Kane et al., 1997; Veigl et al., 1998). Defects in other MMR genes have been implicated in no more than a small proportion of inherited and sporadic cancers. These differences between MMR genes have been attributed to the fact that some MMR proteins have unique functions in MMR, whereas others play partially redundant roles (Harfe and Jinks-Robertson, 2000; Kolodner and Marsischky, 1999; Marsischky et al., 1996). However, some MMR proteins could have different functions, such as, for example, a unique role in DNA damage responses.

Mouse models have provided insight into the relationship between MMR defects and cancer susceptibility (Buermeyer et

SIGNIFICANCE

Tumors that develop in HNPCC patients or sporadic cancers associated with MMR deficiency show increased genomic instability, which can be diagnosed by microsatellite instability (MSI) analysis, and also display resistance to a wide variety of chemotherapeutic agents. A substantial number of HNPCC cases result from missense mutations in MMR genes; however, the functional consequences of such mutations in normal and tumor cells are not well understood. By modeling a human *MSH6* missense mutation in yeast and mice, we demonstrate that MMR missense mutations can differentially affect individual MMR functions. Our results provide new molecular insights into the anticancer functions of MMR and indicate that genotype-phenotype correlations can provide valuable information for the diagnosis and treatment of tumors with MMR mutations.

al., 1999; Wei et al., 2002). Mice that are homozygous for null mutations in *Msh2* or *Mlh1* develop a broad spectrum of tumor types at early ages, and these tumors show MSI; in many regards, these mice mimic HNPCC caused by *MSH2* and *MLH1* mutations (de Wind et al., 1998; Edelmann et al., 1999; Prolla et al., 1998; Reitmair et al., 1996). Mice that are homozygous for *Msh6* mutations are similar to *Msh2* and *Mlh1* mutant mice in regard to tumor spectrum. However, the *Msh6* mutant mice develop cancers at later ages, and the tumors show little or no MSI (Edelmann et al., 1997). Studies of *Msh6* mutant mice were the first to implicate *MSH6* as a late onset cancer susceptibility gene, a result that has been extended to human populations. Pms2 defects in mice cause the development of tumors with MSI at early ages, although the tumor spectrum is distinct from that of *Msh2*, *Msh6*, or *Mlh1* mutant mice (Baker et al., 1995). This difference in tumor spectrum correlates with the limited involvement of *PMS2* defects in HNPCC. Mutations in *Msh3* and *Exo1* only cause the development of tumors at very old ages, which parallels the limited involvement of these genes in HNPCC. However, *Msh3* mutations accelerate the development of tumors when combined with *Msh6* mutations, similar to the interaction between *msh6* and *msh3* mutations in *S. cerevisiae* (de Wind et al., 1999; Edelmann et al., 2000; Kolodner et al., 1999; Marsischky et al., 1996; Sia et al., 1997; Wei et al., 2003).

Mismatch recognition in eukaryotic MMR involves three proteins, MSH2, MSH6, and MSH3, which are homologs of the bacterial MutS protein. These three proteins form two heterodimeric complexes, the MSH2-MSH6 and MSH2-MSH3 complexes, that each have different mismatch recognition properties (Acharya et al., 1996; Drummond et al., 1995; Genschel et al., 1998; Guerrette et al., 1998; Marsischky et al., 1996; Palombo et al., 1995). The MSH2-MSH6 complex is the major mismatch recognition complex and recognizes both base:base and single base insertion/deletion mismatches, whereas the MSH2-MSH3 complex appears to primarily recognize insertion/deletion mismatches. This difference is also reflected in their relative abundance with MSH2-MSH6 complexes occurring in excess of MSH2-MSH3 complexes in yeast, human, and mouse (Marsischky et al., 1996; Genschel et al., 1998; de Wind et al., 1999). It is this difference in mismatch recognition spectrum that has been suggested to underlie the genetic differences between MSH2, MSH6, and MSH3 (Marsischky et al., 1996; Umar et al., 1998). When the MSH complexes bind a mismatch, they form a ring around the DNA, and upon ATP binding, this ring can move along the DNA away from the mismatch (Blackwell et al., 1998; Gradia et al., 1999; Hess et al., 2002). The importance of the ATP binding-mediated release from mispairs has been in part established by the isolation of dominant mutations in *MSH6* in yeast (Das Gupta and Kolodner, 2000). These mutations strongly interfere with MMR when present on a single copy plasmid in a wild-type strain. At the chromosomal locus, they cause high rates of base substitution and frameshift mutations, in contrast to only high rates of base substitution mutations caused by *MSH6* deletion mutations, and the increased rate of frameshift mutations is suppressed by overexpression of *MSH3*. The mutant MSH2-MSH6 complexes hydrolyze ATP in the absence of DNA, but have a much longer half-life bound to a mispair in the presence of ATP than the wild-type complex; the reduced turnover from mispairs may be responsible for preventing MSH2-MSH3 dependent MMR from acting on insertion/deletion mispairs and accounts for the dominant phenotypes caused by these *msh6* mutations (Hess et al., 2002).

Currently, there are two views on how MMR defects lead to increased development of cancer. In one view, increased mutation rates increase the rate of accumulation of mutations in tumor suppressor genes and protooncogenes, which results in the development of cancer (Kinzler and Vogelstein, 1996; Loeb, 2001). In the other, defects in DNA damage responses and DNA damage-induced apoptosis provides a selective advantage to tumor cells (Fishel, 2001; Nowell, 1976; Tomlinson and Bodmer, 1999). To gain insight into these two possible mechanisms, we have investigated the properties of specific single nucleotide changes in *MSH6* in *S. cerevisiae* and mouse models. We describe a dominant mouse *Msh6* mutation that causes a strong mutator phenotype and increased cancer development, but no defect in DNA damage-induced apoptosis, and provide evidence for such mutations in humans. These results indicate that the increased mutation rates resulting from MMR defects are capable of driving the development of cancer, and that certain heterozygous MMR missense mutations can act in a dominant negative manner to increase mutation rates in normal tissue.

Results

Analysis of *MSH6* missense mutations in *S. cerevisiae*

Previous studies described three dominant mutations in the *S. cerevisiae MSH6* gene that cause high rates of both base substitution and frameshift mutations, in contrast to an *msh6* deletion mutation, which only causes high rates of base substitution mutations. Two of the affected amino acids (*S. cerevisiae* codons Ser1036 and Gly1142) are conserved in the human and mouse MSH6 proteins, whereas in one case, Gly1067Asp, the amino acid at the equivalent residue in the human and mouse protein is a Thr (residues 1219 and 1217, respectively). Although the Gly1067Asp substitution is not located in the P loop domain, which is required for ATP binding and processing, molecular modeling indicates that it is situated at the MSH2-MSH6 heterodimer interface close to the P loop of the MSH2 protein (Hess et al., 2002). A recent study reported an MSH6 mutation causing a Thr to Ile change at codon 1219 in an HNPCC case with a tumor with MSI, although little information was presented supporting the pathogenic effects of this mutation (Berends et al., 2002). To study the affect of the Thr and Ile residues on MSH6 function, mutations altering *S. cerevisiae MSH6* codon 1067 to either a Thr or Ile codon were studied both on an ARS CEN plasmid and at the chromosomal *MSH6* locus. On an ARS CEN plasmid in a wild-type strain, the wild-type *MSH6* control and the 1067Thr substitution did not alter the rate of reversion of the *lys2-A10* frameshift mutation (detects deletions in a run of 10 As), whereas the 1067Ile substitution caused a large increase in mutation rate seen in a patch test (Figure 1A). Similar results were obtained using the *CAN1* forward mutation assay (detects gene-inactivating frameshift and base substitution mutations) and the *hom3-10* frameshift reversion assay (detects deletions in a run of 7 Ts) (data not shown). When these plasmids were tested for their ability to complement an *msh6 msh3* double mutant, the wild-type MSH6 control and the MSH6 1067Thr substitution reduced the rate of reversion of the *hom3-10* frameshift mutation similarly, whereas the vector and the MSH6 1067Ile substitution had no effect (Figure 1B). Similar results

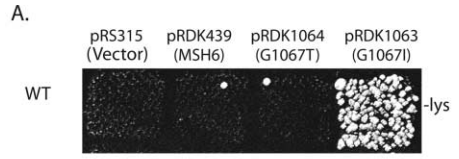

C. Mutation rate analysis

Genotype	Strain	Mutation Rate Hom$^+$	Mutation Rate Can^r
Wild-type	2311	2.8×10^{-9} (1)	8.6×10^{-8} (1)
msh6Δ	3519	1.3×10^{-7} (46)	8.4×10^{-7} (10)
G1067D	3660	1.5×10^{-6} (535)	1.5×10^{-6} (17)
G1067T	5054	9.5×10^{-9} (3)	1.5×10^{-7} (2)
G1067I	5022	1.1×10^{-6} (398)	1.6×10^{-6} (18)

Figure 1. Genetic analysis of *msh6* mutations in yeast

A: The indicated plasmids were transformed into the wild-type strain RDKY 3686, and the presence of a dominant mutator phenotype was detected by determining the relative rate of reversion of the *lys2::InsE-A10* allele by replica plating the strains onto SD plates lacking lysine.

B: The indicated plasmids were transformed into the RDKY 4234 *msh6Δ::hisG msh3Δ::hisG* strain, and complementation of the *msh6Δ::hisG* mutation was detected by determining the relative rate of reversion of the *hom3-10* allele by replica plating the strains onto SD plates lacking threonine.

C: Fluctuation analysis was used to determine the *hom3-10* reversion rate and the *CAN1* forward mutation rate of the indicated strains. The numbers given are the mutation rate followed by the fold increase in mutation rate relative to the wild-type rate in parentheses.

were obtained using the *CAN1* forward mutation assay and the *lys2-A10* frameshift reversion assay (data not shown). Finally, the MSH6 1067Asp, Thr, and Ile substitutions were introduced at the chromosomal *MSH6* locus and tested for their effects on the *CAN1* forward mutation rate and the *hom3-10* frameshift mutation reversion rate (Figure 1C). The MSH6 1067Thr substitution did not significantly increase the mutation rate in either assay compared to the wild-type strain. In contrast, the MSH6 1067Asp and MSH6 1067Ile substitutions had essentially the same effect and increased the *hom3-10* frameshift reversion rate 8- to 10-fold more that the *msh6* deletion mutation, and increased the *CAN1* mutation rate about 2-fold more than the *msh6* deletion mutation; these mutation rates are about 50% of that seen in an *msh2* deletion mutant. These results demonstrate that substituting a Thr for Gly1067 has no effect on MSH6 function, whereas substitution of an Ile at this residue results in loss of MSH6 function and a strong dominant defect in the repair of frameshift mutations as observed for the original dominant *msh6* mutations.

Generation of *Msh6^{T1217D}* mutant mice

We previously generated a mouse line carrying an *Msh6* null allele (*Msh6$^-$*) (Edelmann et al., 1997). *Msh6$^{-/-}$* mice are viable and highly predisposed to the development of tumors. The tumor spectrum in these mice resembles that of MMR-deficient human patients and includes lymphoid tumors, gastrointestinal tumors, and tumors of the skin. Msh6 deficiency causes a defect in the repair of base substitution mutations, but not of 2 bp insertion/deletion mutations. Consequently, the tumors derived from these mice do not display an MSI phenotype. However, a large proportion of *MSH6* mutations in human patients represent missense mutations, whose functional consequences remain unknown (Berends et al., 2002; Kolodner et al., 1999; Wijnen et al., 1999; Wu et al., 1999). We therefore created a mouse line carrying the *Msh6^{T1217D}* mutation to assess the effect of an *Msh6* missense mutation on MMR function and cancer susceptibility (Figures 2A and 2B); the *Msh6^{T1217D}* allele is referred to as *Msh6^{TD}* throughout the manuscript. The *Msh6^{TD}* allele is transmitted in a normal Mendelian ratio, and both heterozygous and homozygous mutant mice develop normally. RT-PCR and Western blot analysis showed that the *Msh6^{TD}* mutation did not interfere with normal gene expression or the stability of the mutant protein (Figures 2C and 2D). In human cells, MSH6 forms a complex with MSH2 to initiate the repair of mispairs, and loss of MSH6 affects the stability of the MSH2 protein (de Leeuw et al., 2000; Palombo et al., 1995). Consistent with this, we detected a reduction of Msh2 protein in *Msh6$^{-/-}$* MEF cells. However, we did not detect a similar reduction in the Msh2 protein levels in *Msh6$^{TD/+}$* or *Msh6$^{TD/TD}$* cell extracts, indicating that the mutation had no effect on the stability of Msh2 protein (Figure 2D). Immunohistochemical analysis also showed that the subcellular distribution of the mutant Msh6^{TD} or Msh2 protein was not affected (data not shown).

Mismatch repair activities in Msh6^{TD} mutant extracts

We next analyzed the effect that the mutant Msh6^{TD} protein had on mismatch recognition and repair in ES cell extracts. Using gel mobility shift assays, we found that extracts of Msh6$^{TD/+}$ and Msh6$^{TD/TD}$ embryonic stem cells contained a G•T mismatch binding activity that was similar to that observed in Msh6$^{+/+}$ extracts (Figure 3A); the activity present in all of the extracts also bound homoduplex DNA, albeit to a lower extent. However, in contrast to Msh6$^{+/+}$ extracts, the G•T binding activity present in both Msh6$^{TD/+}$ and Msh6$^{TD/TD}$ extracts was resistant to ATP-dependent mismatch release, even at high ATP concentrations (see Figure 3A). These results are consistent with previous studies of the corresponding *msh6* mutation in yeast and indicate that the mutant Msh2-Msh6^{TD} complex displays a defect in the modulation of mispair binding and dissociation by ATP (Hess et al., 2002).

To determine the impact of the Msh6^{TD} mutation on DNA repair, we measured the in vitro DNA mismatch repair activity in ES cell extracts using a variety of substrates containing G•G mismatches, single-base insertion, or two-base insertion mismatches with a nick either 5′ or 3′ to the mismatched base (Figure 3B). The Msh6$^{+/+}$ and Msh6$^{TD/+}$ extracts were proficient in the repair of all substrates tested, whereas the Msh6$^{TD/TD}$ extracts did not repair any of these substrates. The repair defect in the Msh6$^{TD/TD}$ extracts differs from the defect previously found in Msh6$^{-/-}$ extracts, which are defective in the repair of base-base mismatches but not single-base insertion and dinucleotide insertion mispairs (Edelmann et al., 1997, 2000). Furthermore, addition of increasing amounts of Msh6$^{TD/TD}$ extracts to Msh6$^{+/+}$ extracts inhibited the repair of dinucleotide insertion mutations

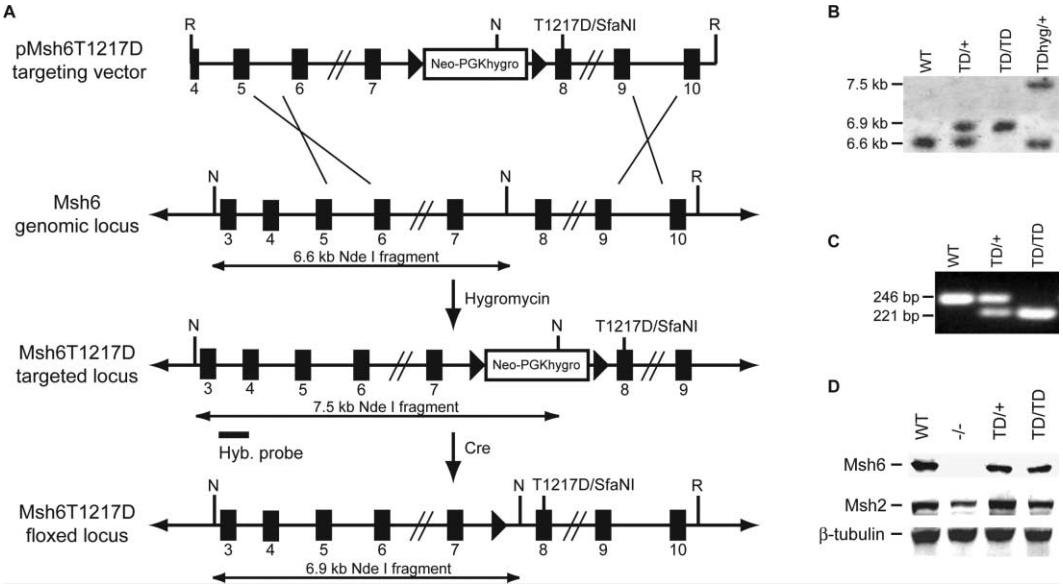

Figure 2. Generation of *Msh6*^{T1217D} mice

A: Gene targeting strategy for the generation of *Msh6*^{T1217D} mice, showing the pMsh6T1217D knockin targeting vector and the wild-type and targeted genomic *Msh6* locus before and after Cre-loxP-mediated deletion of the resistance cassette.

B: Representative Southern blot analysis of NdeI-digested tail genomic DNA from *Msh6* wild-type (WT), heterozygous (TD/+), homozygote (TD/TD), and heterozygote undeleted (TDhyg/+) mice.

C: RT-PCR analysis of total RNA isolated from *Msh6* wild-type (WT), heterozygous (TD/+), and homozygous (TD/TD) mutant ES cells. The TD mutation creates an SfaNI site in the mutant transcript. The RNA transcript in WT mice is resistant to SfaNI digestion (246 bp fragment), while the mutant transcripts in TD/+ and TD/TD mice can be digested into 221 bp and 25 bp (not shown) restriction fragments. The presence of the TD mutation in the RT-PCR products of *Msh6*$^{TD/+}$ and *Msh6*$^{TD/TD}$ mice was further verified by DNA sequencing.

D: Western blot analysis shows expression of stable Msh2 and Msh6 protein in WT, heterozygous (TD/+), and homozygous (TD/TD) mutant MEF cell extracts, while no Msh6 protein and reduced amounts of Msh2 is detected in Msh6-deficient (−/−) extracts.

compared to control assays, in which the same amounts of Msh6$^{-/-}$ extracts were added to Msh6$^{+/+}$ extracts (data not shown). These results demonstrate that in homozygous mutant extracts, the mutant Msh6^{TD} protein interferes with the ability of Msh2-Msh3 complexes to act in repair of dinucleotide insertion/deletion mutations.

Microsatellite instability in *Msh6*^{TD} mutant mice

The repair defect observed in Msh6$^{TD/TD}$ cell extracts suggested that the in vivo mutator phenotype in *Msh6*^{TD} mutant mice would differ from wild-type and also *Msh6*$^{-}$ mice. To assess this, the MSI phenotype was analyzed in tail genomic DNA of *Msh6*$^{+/+}$, *Msh6*$^{-/-}$, *Msh6*$^{TD/+}$, and *Msh6*$^{TD/TD}$ mice at a mononucleotide repeat locus (*U12235*) and two dinucleotide repeat loci (*D7Mit91* and *D17Mit123*) (Figures 4A and 4B). The *Msh6*$^{TD/TD}$ mice displayed a significant increase in MSI at all three loci as compared to *Msh6*$^{+/+}$ mice (Figure 4B). The increase in MSI in the *Msh6*$^{TD/TD}$ was also significant compared to the MSI observed in *Msh6*$^{-/-}$ mice. In addition, the MSI at these loci in *Msh6*$^{TD/TD}$ was comparable to the MSI previously found in *Mlh1*$^{-/-}$ mice (Wei et al., 2003). Interestingly, we also noted a significant increase in MSI in *Msh6*$^{TD/+}$ mice at the *U12235* locus as compared to wild-type mice. The increase in MSI in *Msh6*$^{TD/+}$ mice at the *D7Mit91* locus was of borderline significance and not significant at the *D17Mit123* locus as compared to wild-type mice. These results demonstrate that the *Msh6*^{TD} mutation results in a significant MSI phenotype.

In vivo mutation frequencies and spectra in *Msh6* mutant mice

The analysis of MSI only allows the detection of insertion/deletion mutations and might not reflect all of the features of the mutator phenotype in the *Msh6* mutant mice. Therefore, we analyzed the mutation frequency at the *cII* locus in spleenocytes using the Big Blue transgene system, which allows the analysis of insertion/deletion mutations and base substitutions (Andrew et al., 2000; Kohler et al., 1991). There was a significant increase in mutation frequency in the *Msh6*$^{TD/TD}$ mice and also to a slightly lesser extent in the *Msh6*$^{-/-}$ mice (Figure 5A). The difference between *Msh6*$^{TD/TD}$ and *Msh6*$^{-/-}$ was significant ($p < 0.0001$). Interestingly, this analysis also revealed a 2- to 3- fold increase in the mutation frequency in *Msh6*$^{TD/+}$ mice as compared to wild-type mice ($p < 0.0001$), which was not observed in the *Msh6*$^{+/-}$ mice.

The analysis of the mutation spectra showed that the mutations in *Msh6*$^{+/+}$, *Msh6*$^{+/-}$, and *Msh6*$^{-/-}$ mice were predominantly base substitutions, with a majority of mutations being transitions and only some transversions (Figure 5B). The mutation spectrum in *Msh6*$^{TD/+}$ mice largely resembled the spectrum found in wild-type or *Msh6* null mutant mice. In contrast, in *Msh6*$^{TD/TD}$ mice, almost half of the mutations were single base deletions or insertions. The difference between the mutation spectra in *Msh6*$^{TD/TD}$ and *Msh6*$^{+/+}$ or *Msh6*$^{-/-}$ mice is highly significant (p values < 0.0001), and indicates that the Msh6^{TD} mutation interferes with the repair of insertion/deletion mispairs.

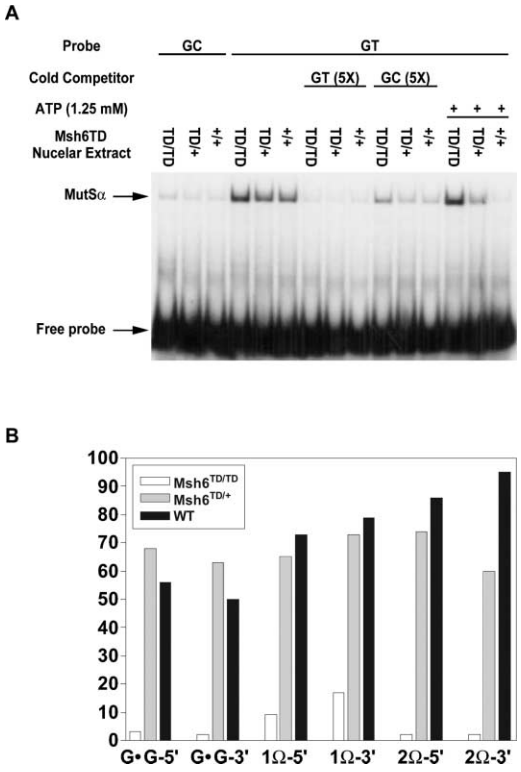

Figure 3. Mismatch repair activities in Msh6 mutant cell extracts

A: Mismatch binding activities of *Msh6*$^{+/+}$, *Msh6*$^{TD/+}$, and *Msh6*$^{TD/TD}$ nuclear extracts. Gel mobility shift assay in Msh6 mutant nuclear extracts was performed by incubating nuclear protein extracts isolated from *Msh6*$^{+/+}$ (+/+), *Msh6*$^{TD/+}$ (TD/+), and *Msh6*$^{TD/TD}$ (TD/TD) ES cells with either GC-containing homoduplex or G/T-containing heteroduplex oligonucleotides. The position of the MutSα-DNA complex and the unbound free probe are indicated by the arrows. Unlabeled (cold) G/T-containing heteroduplex competitor oligonucleotide or ATP was included in the reaction mixture in the molar ratio or concentration indicated.

B: MMR defects in *Msh6*^{TD} mutant cell extracts. DNA mismatch repair activity was assayed in *Msh6*$^{TD/TD}$, *Msh6*$^{TD/+}$, and *Msh6*$^{+/+}$ cell extracts as described (Thomas et al., 1995). Substrates designated with a Ω contain the number of extra nucleotides that accompany the symbol. Substrates are designated 3′ or 5′, indicating the position of the nick relative to the mismatch.

Survival and cancer phenotype in *Msh6*^{TD} mutant mice

To study survival and cancer susceptibility, we followed a cohort of *Msh6*^{TD} mutant mice for a period of up to 24 months. The *Msh6*$^{TD/TD}$ mice had a significantly reduced survival compared to *Msh6*$^{TD/+}$ or wild-type mice (p values < 0.0001; log rank test) (Figure 6). The 50% survival of *Msh6*$^{TD/TD}$ mice was at 12 months of age, and all of the mice died by 20 months of age. Although the overall reduction in survival of *Msh6*$^{TD/TD}$ mice was comparable to *Msh6*$^{-/-}$ mice ($p = 0.91$), there was a significant difference in survival during the first 10 months of life. At this age, more than 80% of *Msh6*$^{TD/TD}$ mice were still alive compared to only 60% of *Msh6*$^{-/-}$ mice ($p < 0.05$). There was also a significant reduction in the survival of *Msh6*$^{TD/+}$ mice compared to their wild-type littermates ($p < 0.004$). While 50% of the *Msh6*$^{TD/+}$ mice died by 20 months of age, more than 80% of wild-type mice were still alive.

The reduction in survival in *Msh6*$^{TD/TD}$ mice was caused by increased cancer susceptibility. To examine the types of tumors present in the *Msh6*$^{TD/TD}$ mutant mice, we analyzed the tumor spectra in 12 mice that were between 7 and 14 months of age. This showed that similar to *Msh6*$^{-/-}$ mice, the majority of *Msh6*$^{TD/TD}$ mice had developed B or T cell non-Hodgkin's lymphomas (11/12 mice) (Figures 7A and 7B) (Edelmann et al., 1997). We also found tumors in the small intestines of the mice, including tubular adenomas (2/12 mice), a tubulovillous adenoma (1/12 mice), and focal areas of dysplasia (4/12 mice) (Figure 7C). Some of the mice also developed basal cell carcinomas of the skin (2/12). We analyzed several of the tumors for the presence of Msh6^{TD} protein either by immunohistochemical analysis (Figure 7D) or Western blot analysis of microdissected tumor tissue (not shown). We found that in all tumors ($n = 4$) that were analyzed, Msh6^{TD} protein could readily be detected. Similarly, immunohistochemical analysis of intestinal tumors showed that while Msh3 was absent in the tumor cells in *Msh3*$^{-/-}$ mice (Figure 7E), Msh3 could readily be detected at normal levels in the tumor cells in *Msh6*$^{TD/TD}$ mice (Figure 7F).

To assess whether the reduction in survival of *Msh6*$^{TD/+}$ mice was associated with increased tumorigenesis, we sacrificed 11 *Msh6*$^{TD/+}$ mice and 10 *Msh6*$^{+/+}$ littermates that were still alive between 17 and 22 months of age. A majority of *Msh6*$^{TD/+}$ mice had developed non-Hodgkin's lymphoma (7/11 mice) at this age, while none of the wild-type mice had detectable tumors. This analysis did not include the *Msh6*$^{TD/+}$ mice that had died previously, and therefore is probably an underestimate of the tumor phenotype. Some of the tumors in the heterozygous mice were also analyzed for the status of the wild-type *Msh6* allele by loss of heterozygosity (LOH) analysis. This showed that in all tumors ($n = 5$) tested, the wild-type allele was retained, indicating that tumor formation in *Msh6*$^{TD/+}$ mice is not associated with LOH at the wild-type allele (data not shown).

The MMR defect observed in *Msh6*$^{TD/TD}$ extracts and the mutator phenotype observed in normal tissue of *Msh6*^{TD} mutant mice suggested the tumors in *Msh6*^{TD} mice would show MSI. Indeed, we found that tumors in both *Msh6*$^{TD/TD}$ homozygous and *Msh6*$^{TD/+}$ heterozygous mice displayed an MSI phenotype (Figures 7G–7J). In *Msh6*$^{TD/TD}$ mice, 5 of 9 (5/9) tumors analyzed were unstable at *D7Mit91*, 3/9 tumors were unstable at *D17Mit123*, and 7/9 tumors were unstable at *U12235*. A similar analysis in *Msh6*$^{TD/+}$ mice showed that 2/5 tumors were unstable at *D7Mit91*, 1/5 tumors at *D17Mit123*, and 1/5 tumors at *U12235*.

DNA damage response in *Msh6*$^{TD/TD}$ MEF cells

Numerous studies have indicated that MMR not only repairs mismatched bases, but also mediates an apoptotic response after exposure of cells to DNA damaging agents (Buermeyer et al., 1999; Li, 1999; Modrich, 1997). In addition, tumor cell lines or mouse cell lines that are deficient in either MSH2 or MSH6 display increased resistance to the cytotoxic effect of a variety of genotoxic agents (de Wind et al., 1999; Drummond et al., 1995; Fink et al., 1997; Umar et al., 1997; Zhang et al., 1999). To study the effect of the Msh6^{TD} mutation on this MMR function, we established *Msh6*$^{+/+}$, *Msh6*$^{-/-}$, and *Msh6*$^{TD/TD}$ MEF strains and analyzed their response to exposure to several DNA damaging agents. *Msh6*$^{-/-}$ cells were resistant to the genotoxic effects of cisplatin at the drug levels tested. In contrast, *Msh6*$^{TD/TD}$ cells were as sensitive to cisplatin treatment as *Msh6*$^{+/+}$ cells (Figures 8A and 8B). The difference in cisplatin sensitivity between *Msh6*$^{-/-}$ and *Msh6*$^{+/+}$ or *Msh6*$^{TD/TD}$ cells was highly significant ($p < 0.0001$). Similarly, *Msh6*$^{-/-}$ cells were largely resistant to

A.

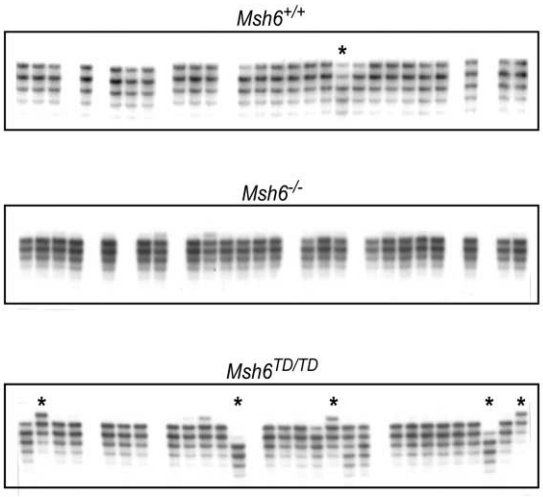

Figure 4. MSI in genomic DNA of *Msh6* mutant mice

A: Genomic DNA from wild-type (*Msh6*$^{+/+}$), *Msh6* null (*Msh6*$^{-/-}$), and *Msh6*^{TD} homozygous mutant mice (*Msh6*$^{TD/TD}$) was analyzed for MSI at marker *D7Mit91*. Asterisks indicate unstable alleles.

B: Comparison of MSI in *Msh6* mutant mouse lines.

B. Comparison of MSI in genomic DNA of *Msh6* mutant mice

Marker	*Msh6*$^{+/+}$	*Msh6*$^{-/-}$	*Msh6*$^{TD/+}$	*Msh6*$^{TD/TD}$	*Mlh1*$^{-/-}$ [1]
U12335 (A)n	5% (5/102)	9% (6/68)	15% (16/108)[2]	22% (24/108)[4,5]	16% (12/73)
D7Mit91 (CA)n	2% (3/124)[1]	3% (3/100)	8% (14/182)[3]	12% (19/158)[4,5]	15% (19/123)
D17Mit123 (CA)	4% (4/99)	6% (8/132)	10% (11/116)	14% (19/141)[4,5]	28% (19/69)

Mutation frequency was determined as the number of unstable alleles divided by the number of total alleles scored.
[1]data from Wei et al., 2003. *Msh6*$^{TD/+}$ versus *Msh6*$^{+/+}$: [2]p-value < 0.05, [3]p-value = 0.073; *Msh6*$^{TD/TD}$ versus *Msh6*$^{+/+}$: [4]p-value < 0.05; *Msh6*$^{TD/TD}$ versus *Msh6*$^{-/-}$: [5]p-value < 0.05, Fisher's exact test.

treatment with MNNG or 6-TG, while *Msh6*$^{TD/TD}$ cells remained as sensitive to treatment with these agents as *Msh6*$^{+/+}$ cells (Figures 8D and 8E and Figures 8G and 8H, respectively). Furthermore, the sensitivity of the *Msh6*$^{+/+}$ and *Msh6*$^{TD/TD}$ cells to all three DNA-damaging agents was associated with a significant increase in the number of apoptotic cells as compared to untreated cells (p values $<$ 0.0001) (Figures 8C, 8F, and 8I). In contrast, no significant increase in the number of apoptotic cells was seen with *Msh6*$^{-/-}$ cells under these conditions. These results indicate that although the Msh6^{TD} mutation causes DNA repair deficiency, it does not affect the apoptotic response to DNA damage.

Discussion

Previous studies in yeast have defined a number of novel dominant missense mutations in *MSH6* that cause a stronger mutator phenotype than deletion of *MSH6* (Das Gupta and Kolodner, 2000). We have investigated whether the equivalent of one such mutation, resulting in the amino acid substitution Thr1217Asp, would be dominant in the mouse, and what the phenotypic consequences of such a mutation might be. Extensive analysis of both ES cells and normal mouse tissues containing this mutation indicate that it causes dominant defects in MMR similar to those caused by the yeast mutation. The mouse Thr1217Asp amino acid substitution resulted in an MSH2-MSH6 complex that could bind mispaired bases but was resistant to ATP-induced release. In vitro, the homozygous mutation resulted in a defect in the repair of dinucleotide insertion/deletion mispairs, in contrast to an *Msh6* deletion mutation, which does not cause such defects. In addition, in normal mouse tissues, the homozygous *Msh6*^{TD} mutation caused both dinucleotide repeat instability and increased frameshift mutations in a reporter transgene, in contrast to the weaker mutator phenotype caused by an *Msh6* deletion mutation. Normal tissues that were heterozygous for the *Msh6*^{TD} mutation also showed increased MSI and accumulation of mutations in the reporter transgene. The homozygous mutant *Msh6*^{TD} mice had a cancer susceptibility phenotype which was similar to that caused by an *Msh6* deletion mutation, except that the tumors showed dinucleotide repeat instability in contrast to an absence of dinucleotide repeat instability in tumors from *Msh6* deletion mutant animals (Edelmann et al., 1997). Importantly, the heterozygous *Msh6*^{TD} missense mutant mice had significantly increased cancer susceptibility predicted to result from a dominant mutation. Consistent with this, a human *MSH6* mutation resulting in the substitution of Ile at the equivalent amino acid reported in a suspected HNPCC case associated with dinucleotide repeat instability was a dominant

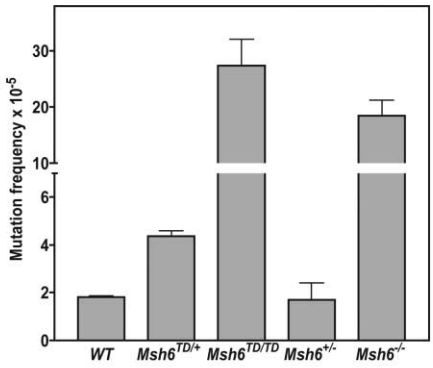

B. Mutation spectrum in spleenocytes of *Msh6* mutant mice

Mutation	*Msh6*$^{+/+}$	*Msh6*$^{+/-}$	*Msh6*$^{TD/-}$	*Msh6*$^{-/-}$	*Msh6*$^{TD/TD}$
Base substitution	**17 (89%)**	**16 (84%)**	**44 (80%)**	**33 (83%)**	**37 (51%)**[1,2]
Transitions	10 (53%)	11 (58%)	29 (53%)	27 (68%)	30 (41%)
Transversions	7 (36%)	5 (26%)	15 (27%)	6 (15%)	7 (10%)
Deletion/Insertion	**2 (11%)**	**3 (16%)**	**11 (20%)**	**7 (17%)**	**36 (49%)**[1,2]
1 bp deletion	1 (5%)	2 (11%)	9 (16%)	7 (17%)	28 (38%)
1 bp insertion	1 (5%)	1 (5%)	2 (4%)	0	6 (8%)
Other mutations	0	0	0	0	2 (3%)
Total	19 (100%)	19 (100%)	55 (100%)	40 (100%)	73 (100%)

[1] *Msh6*$^{TD/TD}$ versus *Msh6*$^{+/+}$, p-value < 0.0001; [2] *Msh6*$^{TD/TD}$ versus *Msh6*$^{-/-}$, p-value < 0.0001.

Figure 5. Increased mutation frequencies in *Msh6* mutant mice

A: Comparison of mutation frequencies at the *cII* locus in *Msh6* mutant mice.
B: Comparison of *cII* mutation spectra in *Msh6* mutant mice.

mutation when modeled in yeast. These results illustrate the complementary insights that can be obtained through the analysis of yeast, mouse, and human systems.

The analysis of microsatellite instability in human tumors indicates that in contrast to tumors with *MSH2* or *MLH1* mutations, mutations in *MSH6* are often associated with a low microsatellite instability phenotype (MSI-L) at dinucleotide markers

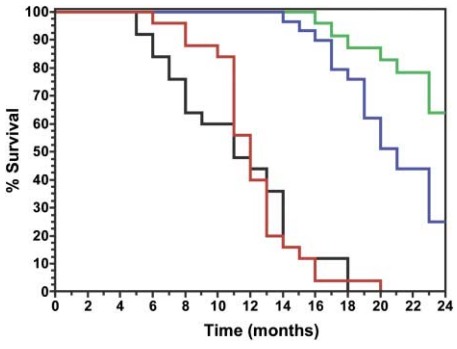

Figure 6. Reduced survival of *Msh6*^{TD} mutant mice

The time of death or the time when the mice became moribund was recorded. The survival curves were generated by using GraphPad Prism 3.0 software. Statistical analysis was performed according to log-rank test. Solid green line, *Msh6*$^{+/+}$ mice (n = 25); solid blue line, *Msh6*$^{TD/+}$ mice (n = 29); solid red line, *Msh6*$^{TD/TD}$ mice (n = 25); solid black line, *Msh6*$^{-/-}$ mice (n = 25).

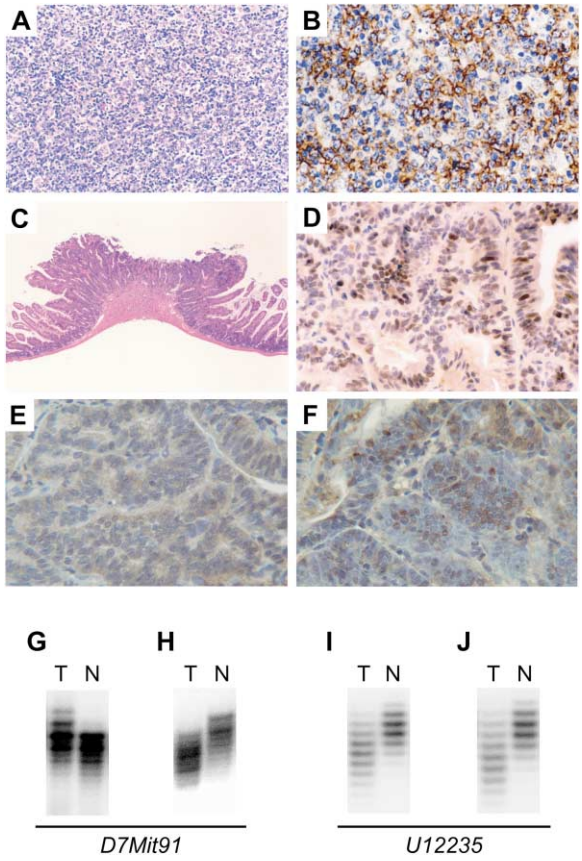

Figure 7. Tumors in *Msh6*^{TD} mutant mice

A: Section of mesenteric lymphoma in an *Msh6*$^{TD/TD}$ mouse. Histologically it was classified as diffuse non-Hodgkin's lymphoma, mixed large noncleaved and cleaved cell type. (200×).
B: Section of mesenteric lymphoma stained with a B cell-specific antibody (400×).
C: Adenoma in the small intestine of an *Msh6*$^{TD/TD}$ mouse. Histological features showed that the tumor was composed of glandular structures (40×).
D: Section of intestinal tumor in an *Msh6*$^{TD/TD}$ mouse stained with an Msh6 specific monoclonal antibody. The Msh6 protein expression was mostly detected in nuclei of tumor cells (400×).
E: Section of intestinal tumor in an *Msh3*$^{-/-}$ mouse stained with an Msh3 specific monoclonal antibody. The Msh3 protein expression was absent in tumor cells (400×).
F: Section of intestinal tumor in an *Msh6*$^{TD/TD}$ mouse stained with an Msh3 specific monoclonal antibody. The Msh3 protein expression was mostly detected in the nuclei of tumor cells (400×).
G and H: MSI at dinucleotide marker *D7Mit91* in an *Msh6*$^{TD/TD}$ GI adenoma (**G**) and an *Msh6*$^{TD/+}$ lymphoma (**H**).
I and J: MSI at mononucleotide marker *U12235* in an *Msh6*$^{TD/TD}$ GI adenoma (**I**) and an *Msh6*$^{TD/TD}$ lymphoma (**J**).

(Akiyama et al., 1997; Kolodner et al., 1999; Verma et al., 1999; Wijnen et al., 1999; Wu et al., 1999). However, in recent studies of suspected HNPCC cases with *MSH6* missense mutations, several tumors have been identified that display high microsatellite instability (MSI-H) (Berends et al., 2002). Our studies with *Msh6*$^{-/-}$ and *Msh6*$^{TD/TD}$ mutant mice provide an explanation for these differences and indicate a genotype-phenotype correlation for this type of genetic instability in *MSH6* mutant tumor cells. In *Msh6*$^{-/-}$ tumors, the lack of Msh6 protein does not interfere with the function of the Msh2-Msh3 heterodimer, while the presence of the mutant Msh6^{TD} protein in tumor cells appar-

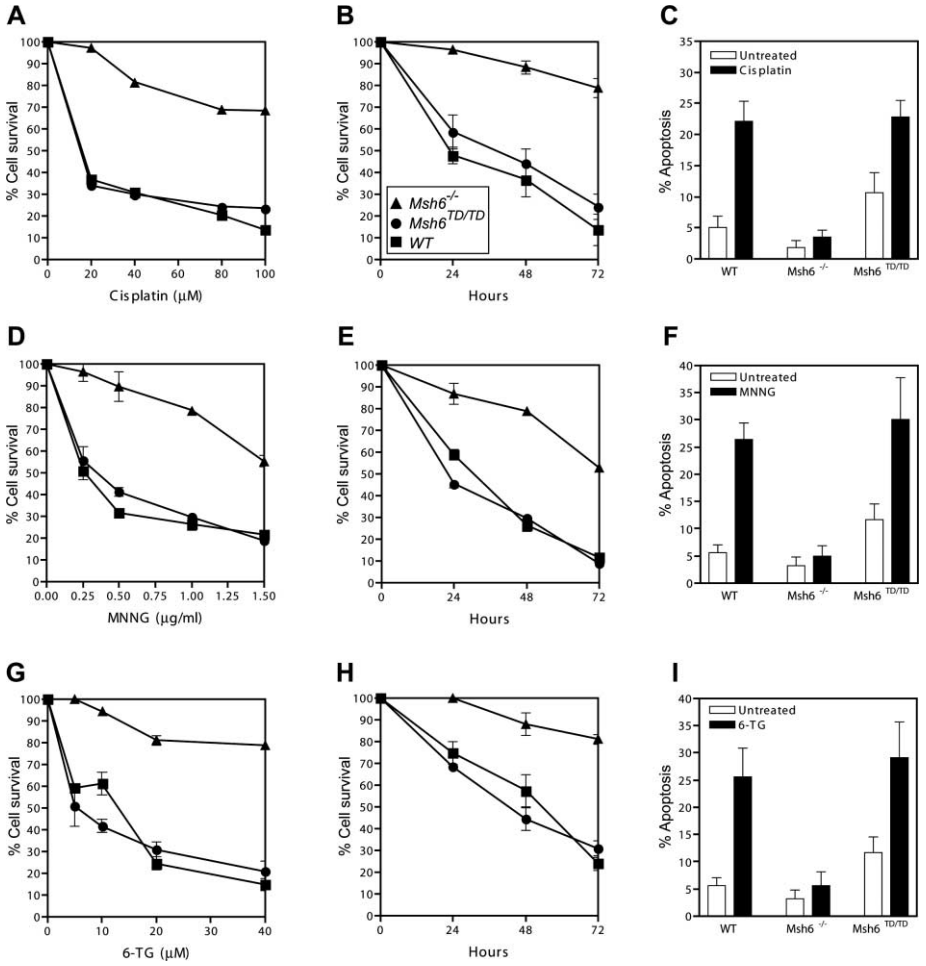

Figure 8. Drug sensitivity and apoptosis in *Msh6* mutant cells

MEF strains of the different *Msh6* genotypes were exposed to cisplatin, MNNG, and 6-TG at varying concentrations and for different time periods.
A: Survival of cells after 48 hr exposure at different cisplatin concentrations.
B: Survival of cells after exposure to 80 μM cisplatin at different time intervals.
C: Apoptotic response to cisplatin treatment (20 μM cisplatin for 24 hr).
D: Survival of cells after 48 hr exposure at different MNNG concentrations.
E: Survival of cells after exposure with 1.0 μg/ml MNNG at different time intervals.
F: Apoptotic response to MNNG treatment (1.0 μg/ml MNNG for 24 hr).
G: Survival of cells after 72 hr exposure at different 6-TG concentrations.
H: Survival of cells after exposure with 20 μM 6-TG at different time intervals.
I: Apoptotic response to 6-TG treatment (10 μM 6-TG for 24 hr).

ently interferes with the Msh2-Msh3 mediated repair of dinucleotide insertion/deletion mutations, paralleling the impairment of the repair of insertion/deletions in nuclear extracts. This predicts that in *Msh6* mutant tumors that display an MSI-H phenotype, the mutant Msh6 protein will be retained. In addition, loss of MSH3 protein is not required for the MSI phenotype. Indeed, we observed that all of the tumors tested in the mouse remained positive for Msh6 and Msh3 immunostaining. Our results are consistent with a recent study of *MSH6* tumors in human HNPCC and HNPCC-like patients that documented MSI-H colorectal and endometrial tumors that were positive for MSH6 staining and MSI-L tumors that were negative for MSH6 staining (Berends et al., 2002). Furthermore, the human MSH6 Thr1219Ile mutation found to be a dominant mutation in yeast was identified in a suspect HNPCC case with an MSI-H tumor. It is therefore likely that the MSI phenotype in *MSH6* mutant tumors is a function of the type of *MSH6* mutation and the stability of the mutant MSH6 protein present in the tumor cells. It should be noted that in cases where MSH6 is not expressed, an MSI-H phenotype can occur due to a secondary mutation in *MSH3*, a phenomenon seen in both yeast and a small number of suspected HNPCC cases (Akiyama et al., 1997; Marsischky et al., 1996; Sia et al., 1997).

Other important roles for MMR in addition to the correction of mispaired bases have been recognized. One of these functions is the processing of DNA damage and the subsequent induction of an apoptotic response. As a consequence, mammalian cells deficient in MSH2, MSH6, MLH1, and PMS2 display resistance to DNA-damaging agents such as 6-TG, cisplatin, and MNNG (Buermeyer et al., 1999; de Wind et al., 1999; Drummond et al., 1995; Duckett et al., 1996; Fink et al., 1997; Fishel, 2001; Koi et al., 1994; Li, 1999; Modrich, 1997; Umar et al., 1997). Complementation by chromosome transfer of *MSH2*, *MSH6*, and *MLH1* reversed the resistance phenotype in mammalian cells and clearly implicated the MMR system in this response (Koi et al., 1994; Umar et al., 1997). Because the Msh2-Msh6 complex recognizes DNA adducts such as O^6-methylguanine and cisplatin adducts, it has been suggested that MMR proteins may act in sensing DNA damage and also directly participate in the processing of damaged DNA residues (Fishel, 2001; Li, 1999; Modrich, 1997). Several different models have been developed to explain the role of MMR proteins in DNA damage responses. In one model, DNA repair-competent cells engage in futile repair cycles after treatment with alkylating agents, and these futile repair cycles lead to the formation of double strand breaks that signal cell cycle arrest and apoptosis (Karran and Bignami, 1994). Alternatively, it has been suggested that MMR proteins may function as damage sensors directly linked to apoptotic responses via a signal transduction cascade or indirectly linked by binding to damaged bases, which subse-

quently blocks DNA replication or other processes, such as transcription and repair, leading to cell death (Fishel, 2001; Li, 1999; Modrich, 1997). The finding that the mutant Msh2-Msh6^{TD} complex does not function in MMR but is still capable of mismatch binding and of initiating apoptosis in response to cisplatin, MNNG, and 6-TG exposure supports the idea that Msh2-Msh6 complexes can function as DNA damage sensors and suggest that excision of DNA lesions is not required for the DNA damage response function of MMR.

While it is generally accepted that an increase in mutation rate due to MMR defects is an important factor underlying tumorigenesis, the importance of defects in MMR-mediated DNA damage-induced apoptosis remains unclear. It has been proposed that mutations in MMR genes, which result in resistance to DNA damage-induced apoptosis, provide a selective advantage in the initial stages of tumorigenesis (Fishel, 2001). In this model, inactivation of MMR and the resulting increased mutation rates accelerate tumorigenesis but are not the origin of it. The observation that *Msh6*$^{-/-}$ ES cells, but not *Msh3*$^{-/-}$ ES cells, display resistance to MNNG is consistent with the unique involvement of Msh2-Msh6 (but not Msh2-Msh3) in DNA damage response (de Wind et al., 1999), and it was suggested that this difference in function may explain the prevalence of mutations in *MSH2* and *MSH6* but not *MSH3* in HNPCC tumors (Heinen et al., 2002). In addition, it was suggested that the tissue selectivity of HNPCC tumors might be traced to exposure to certain types of DNA damaging processes such as alkylation or oxidation in target tissues (Fishel, 2001). The analysis of *Msh6*$^{-/-}$ and *Msh6*$^{TD/TD}$ mice indicates that the apparently normal DNA damage response in *Msh6*$^{TD/TD}$ mutant mice did delay the onset of tumorigenesis during the first 10 months of life. However, it did not alter either the overall survival or tumor spectrum of *Msh6*$^{TD/TD}$ mice as compared to *Msh6*$^{-/-}$ mice. This suggests that the increased mutator phenotype in the mice is sufficient to drive tumorigenesis regardless of the status in DNA damage response function. In a similar analysis of mice with an Msh2^{G674A} missense mutation, which were MMR-deficient but retained normal apoptotic signaling, we also observed a strong cancer phenotype (Lin et al., 2004). Like the *Msh6*$^{TD/TD}$ mice, the *Msh2*$^{G674A/G674A}$ mice also showed a delayed tumor onset as compared to *Msh2*$^{-/-}$ mice, suggesting that the DNA damage response function in these mice could inhibit tumorigenesis at an early stage. However, the age of tumor onset of both *Msh6*$^{TD/TD}$ and *Msh6*$^{-/-}$ mice is delayed compared to *Msh2*$^{-/-}$ and *Msh2*$^{G674A/G674A}$ mice, which is possibly due to a stronger mutator phenotype in the *Msh2* mutant mice. A similar relative mutator phenotype is seen in yeast (Das Gupta and Kolodner, 2000). Based on these studies in mice, it seems likely that the MMR functions in DNA repair and apoptosis cooperate in tumor suppression, but that the increase in mutation rates resulting from MMR defects is sufficient to drive tumorigenesis. Unfortunately, it has not yet been possible to identify mutations in MMR genes that inactivate apoptosis but not DNA repair to evaluate whether defects in MMR-induced apoptosis also can drive tumorigenesis. One implication of the observation that MMR missense mutations can differentially affect DNA repair and MMR-induced apoptosis is that the clinical characteristics of HNPCC caused by missense mutations may be more heterogeneous than those caused by complete loss of function mutations. In addition, human tumors with certain *MSH6* missense mutations will display MSI and may remain responsive to treatment with chemotherapeutic agents. Therefore, determining the genotype/phenotype correlations of *MSH6* missense mutations may provide valuable information for prevention, treatment, and prognosis of individuals with such mutations.

Experimental procedures

Yeast procedures

All yeast genetics methods have been described in detail (Amin et al., 2001; Das Gupta and Kolodner, 2000; Marsischky et al., 1996). Yeast cells were grown in YEPD or synthetic dropout (SD) medium with or without 2% bactoagar. SD medium was supplemented with the appropriate dropout mix of amino acids (BIO101, Inc., Vista, CA), and canavanine plates were SD arginine medium supplemented with 60 mg/l of canavanine (SIGMA, St. Louis, MO). Transformations were performed using standard procedures. Mutations were placed at the chromosomal *MSH6* locus using standard pop-in, pop-out procedures, and then the *MSH6* gene present in each strain was amplified by PCR and sequenced to verify the presence of the desired mutation and the lack of additional mutations. Patch tests to identify mutator phenotypes were performed as described (Amin et al., 2001), and mutation rates were determined by fluctuation analysis using at least 14 independent cultures as described (Amin et al., 2001; Das Gupta and Kolodner, 2000; Lea and Coulson, 1948; Marsischky et al., 1996).

The yeast strains used in patch tests were isogenic derivatives of S288C (Amin et al., 2001). The wild-type strain was RDKY 3686 *MAT*α *ura3-52 leu2Δ1 trp1Δ63 his3Δ200 hom3-10 lys2::InsE-A10*, and the *msh3 msh6* double mutant was a derivative RDKY 4234 that also contained the *msh6Δ::hisG msh3Δ::hisG* mutations (Marsischky et al., 1996). The strain background used for analysis of the effect of chromosomal *msh6* mutations on mutation rates is RDKY 2311 *MAT*a *trp1 ura3-52 ade2-1 hom3-10 leu2-3112*. RDKY 2311 and the mutant derivatives RDKY 3519 *msh6Δ::hisG* and RDKY 3660 *msh6-G1067D* have been described (Das Gupta and Kolodner, 2000). The derivatives RDKY 5054 *msh6-G1067T* and RDKY 5022 *msh6-G1067I* were constructed for this study using *URA3* integrative plasmids containing the *msh6-G1067T* and *msh6-G1067I* mutations, respectively.

The plasmids used were constructed as follows. pRS315 is a standard *ARS CEN LEU2* cloning vector, and pRDK439 is a derivative from our lab collection containing a genomic *MSH6* fragment spanning the BamHI site upstream of the *MSH6* promoter to the first HindIII site downstream of MSH6 inserted into BamHI, HindIII-cut pRS315 (Das Gupta and Kolodner, 2000). The msh6-G1067T and msh6-G1067I mutations were introduced with the QuickChange Site-Directed Mutagenesis kit (Stratagene), and the resulting plasmids were fully sequenced. *URA3* integrative plasmid derivatives were then constructed by subcloning the BamHI, HindIII fragment into pRS306.

Generation of *Msh6*^{TD} mutant mice

A 10 kb EcoRI fragment containing the *Msh6* region surrounding exon 8 was isolated from a 129SvEv BAC genomic library and subcloned into pBluescript. A mutation was introduced that changed codon 1217 from threonine (ACC) to aspartic acid (GAT) by site-directed mutagenesis (Stratagene Quick Change Kit) and verified by sequencing. A 5.0 kb NotI fragment containing two loxP sites flanking a neomycin-PGKhygromycin resistance cassette was sublconed into a single Bsu36I site in intron 7. The targeting vector was linearized by NotI restriction digestion and electroporated into WW6 embryonic stem cells (Edelmann et al., 1997). Four correctly targeted ES cell lines were injected into C57BL/6J blastocysts. Male chimeras that resulted from these injections were mated to C57BL/6J females and transmitted the mutant allele through their germline. F1 males carrying the mutant allele were mated to *Zp3Cre* transgenic females (C57BL/6J) to remove the resistance cassette by LoxP-mediated recombination. Male and female mice carrying the modified allele were intercrossed to generate *Msh6*$^{+/+}$, *Msh6*$^{TD/+}$, and *Msh6*$^{TD/TD}$ mutant mice.

RT-PCR analysis

Total RNA was isolated from *Msh6*^{TD} mutant ES cell lines using the RNeasy purification Kit (Qiagen). RT-PCR was performed using forward primer: 5′-AAGACAGGCTGGTCTGTTGG-3′ and reverse primer: 5′-GCTGTCCCAT CAAAAGTTGC-3′ using the Titan One Tube-RT-PCR reaction kit (Roche) according to the manufacturers instruction. The resulting 246 bp fragment was digested with SfaNI to detect the presence of the mutant RNA transcript.

Western blot analysis

MEF cell extracts were prepared according to standard procedures, and 50 μg protein of each cell lysate was separated on a 10% SDS-PAGE gel. Protein was transferred onto PROTRAN membranes, and the membranes were subsequently incubated with monoclonal antibodies directed against Msh2 (Ab-2, Oncogene), Msh6 (clone 44, BD Biosciences), and rabbit polyclonal antibody directed against β-tubulin (H-235, Santa Cruz).

Gel mobility shift assays

Nuclear extracts were prepared as described (Dignam et al., 1983). The invariant sense oligonucleotide 5′-GGGAAGCTGCCAGGCCCCAGTGTCAG CCTCCTATGCTC-3′ was end-labeled with γ^{32}-ATP and annealed in 1× DNA binding buffer (12% glycerol, 20 mM HEPES [pH 7.9], 100 mM KCl, 1 mM DTT, and 5 mM $MgCl_2$) with 3× molar ratios of antisense oligonucleotide (5′-GAGCATAGGAGGCTGACACTGGGGCCTGGCAGCTTCCC-3′ to form a GC homoduplex probe) or with 3× molar ratios of antisense oligonucleotide (5′-GAGCATAGGAGGCTGACATTGGGGCCTGGCAGCTTCCC-3′) to form a GT mismatch-containing heteroduplex probe. Ten μg of nuclear extract was preincubated in 1× DNA binding buffer, 1 μg dIdC, and 20 ng unlabeled homoduplex for 5 min on ice in a total volume of 19 μl. Twenty ng of radiolabeled DNA probe was subsequently added, and the binding mixture was incubated on ice for 30 min. For reaction using cold probe competition, cold competitor (100 ng) was included in the preincubation mixture. For adenine nucleotide challenge experiments, ATP was added 15 min after addition of the DNA probe. The reaction mixture was then subjected to electrophoresis in a 5% polyacrylamide gel in 0.5× TBE buffer containing 2.5% glycerol. The gels were dried and autoradiographed.

Cell-free extracts and mismatch repair assay

Procedures for extract and heteroduplex substrate preparation and for measuring repair activity were as described (Thomas et al., 1995). The substrates used are described in the legend to Figure 3B.

MSI analysis

Mutations in microsatellite sequences were assayed by PCR of single target molecules. Equal amounts of tail DNA from ten mice per mouse strain (*Msh6*$^{+/+}$, *Msh6*$^{-/-}$, *Msh6*$^{TD/+}$, and *Msh6*$^{TD/TD}$) were pooled and diluted to 0.5 to 1.0 genome equivalents. Cycling reactions for the three markers analyzed, *U12235*, *D7Mit91*, and *D17Mit123*, were performed as described previously (Wei et al., 2003).

In vivo mutation analysis

The in vivo mutation frequency in spleenocytes of WT and *Msh6* mutant mice was assessed using the target *cII* transgene in the Big Blue Transgenic Rodent Mutagenesis Assay System (Stratagene) according to the manufacturer's guidelines. Three mice each from *Msh6*$^{+/+}$*/Big Blue, Msh6*$^{+/-}$*/BigBlue, Msh6*$^{-/-}$*/Big Blue, Msh6*$^{TD/+}$*/Big Blue*, and *Msh6*$^{TD/TD}$*/Big Blue* mouse strains were sacrificed at 10 weeks of age and analyzed. To characterize the *cII* locus in mutant phage particles, the entire *cII* gene was PCR amplified and sequenced. Statistical analysis was performed using the Fisher's exact test.

Analysis of tumors

Tumors from sacrificed mice were removed and fixed in 10% neutral buffered formalin. All tumors were processed for paraffin embedding, and sections were prepared for staining with hematoxylin and eosin according to standard procedures. For immunohistochemical analysis, the tumor sections were deparaffinized and stained with antibodies for immunotyping (B lymphocyte CD45R/B220 [Pharmingen] and T lymphocyte CD3 [Vector and Zymed]) or antibodies directed against Msh6 (clone 44, BD Biosciences) and Msh3 (clone 52, BD Transduction Laboratories). Statistical analyses of tumor incidence was performed using the Fisher's exact test.

MEF survival analysis

MEF cells (5×10^4) of each *Msh6* genotype were exposed to cisplatin, 6-TG, or MNNG at different drug concentrations or for different time periods. After drug exposure, the cells were washed once with PBS, once with PBS:Methanol (1:1), and fixed in 0.5 ml 100% methanol. The cells were air dried, stained with 0.1% crystal violet, and extensively washed with PBS, and the dye extracted in 10% acetic acid. The dye concentration was determined by measuring absorption at A_{600} nm, and the percentage cell survival was calculated as (treated cells/untreated cells) × 100. The apoptotic response to drug exposure was measured by TUNEL (DeadEnd Fluorometric TUNEL System, Promega). All experiments were performed for three different MEF strains for each *Msh6* genotype and repeated at least three times for each strain. Cisplatin (Bedford Laboratories), 6-TG (Sigma), and MNNG (Sigma) dilutions in culture medium were prepared fresh before use. For the exposure to MNNG, 20 μM O^6-benzylguanine (Sigma) was added to the medium.

Acknowledgments

This work was supported by the National Institutes of Health (CA76329 and CA93484 to W.E., GM50006 to R.D.K., ES11040 and CA84301 to R.K., and center grant CA13330 to the Albert Einstein College of Medicine), a Deutsche Krebshilfe fellowship (to S.J.S.), and an Irma T. Hirschl Career Scientist Award (to W.E.).

Received: January 23, 2004
Revised: May 6, 2004
Accepted: June 17, 2004
Published: August 23, 2004

References

Acharya, S., Wilson, T., Gradia, S., Kane, M.F., Guerrette, S., Marsischky, G.T., Kolodner, R., and Fishel, R. (1996). hMSH2 forms specific mispair-binding complexes with hMSH3 and hMSH6. Proc. Natl. Acad. Sci. USA *93*, 13629–13634.

Aebi, S., Kurdi-Haidar, B., Gordon, R., Cenni, B., Zheng, H., Fink, D., Christen, R.D., Boland, C.R., Koi, M., Fishel, R., and Howell, S.B. (1996). Loss of DNA mismatch repair in acquired resistance to cisplatin. Cancer Res. *56*, 3087–3090.

Akiyama, Y., Sato, H., Yamada, T., Nagasaki, H., Tsuchiya, A., Abe, R., and Yuasa, Y. (1997). Germ-line mutation of the hMSH6/GTBP gene in an atypical hereditary nonpolyposis colorectal cancer kindred. Cancer Res. *57*, 3920–3923.

Amin, N.S., Nguyen, M.N., Oh, S., and Kolodner, R.D. (2001). exo1-Dependent mutator mutations: Model system for studying functional interactions in mismatch repair. Mol. Cell. Biol. *21*, 5142–5155.

Andrew, S.E., Xu, X.S., Baross-Francis, A., Narayanan, L., Milhausen, K., Liskay, R.M., Jirik, F.R., and Glazer, P.M. (2000). Mutagenesis in PMS2- and MSH2-deficient mice indicates differential protection from transversions and frameshifts. Carcinogenesis *21*, 1291–1295.

Baker, S.M., Bronner, C.E., Zhang, I., Plug, A., Robatzek, M., Warren, G., Elliott, E.A., Yu, J., Ashley, T., Arnheim, N., et al. (1995). Male mice defective in the DNA mismatch repair gene *PMS2* exhibit abnormal chromosome synapsis in meiosis. Cell *82*, 309–320.

Berends, M.J., Wu, Y., Sijmons, R.H., Mensink, R.G., van der Sluis, T., Hordijk-Hos, J.M., de Vries, E.G., Hollema, H., Karrenbeld, A., Buys, C.H., et al. (2002). Molecular and clinical characteristics of MSH6 variants: An analysis of 25 index carriers of a germline variant. Am. J. Hum. Genet. *70*, 26–37.

Bignami, M., Casorelli, I., and Karran, P. (2003). Mismatch repair and response to DNA-damaging antitumour therapies. Eur. J. Cancer *39*, 2142–2149.

Blackwell, L.J., Martik, D., Bjornson, K.P., Bjornson, E.S., and Modrich, P. (1998). Nucleotide-promoted release of hMutSalpha from heteroduplex DNA is consistent with an ATP-dependent translocation mechanism. J. Biol. Chem. *273*, 32055–32062.

Buermeyer, A.B., Deschênes, S.M., Baker, S.M., and Liskay, R.M. (1999). Mammalian mismatch repair. Annu. Rev. Genet. *33*, 533–564.

D'Atri, S., Tentori, L., Lacal, P.M., Graziani, G., Pagani, E., Benincasa, E., Zambruno, G., Bonmassar, E., and Jiricny, J. (1998). Involvement of the

mismatch repair system in temozolomide-induced apoptosis. Mol. Pharmacol. *54*, 334–341.

Das Gupta, R., and Kolodner, R.D. (2000). Novel dominant mutations in Saccharomyces cerevisiae MSH6. Nat. Genet. *24*, 53–56.

de Leeuw, W.J., Dierssen, J., Vasen, H.F., Wijnen, J.T., Kenter, G.G., Meijers-Heijboer, H., Brocker-Vriends, A., Stormorken, A., Moller, P., Menko, F., et al. (2000). Prediction of a mismatch repair gene defect by microsatellite instability and immunohistochemical analysis in endometrial tumours from HNPCC patients. J. Pathol. *192*, 328–335.

de Wind, N., Dekker, M., van Rossum, A., van der Valk, M., and te Riele, H. (1998). Mouse models for hereditary nonpolyposis colorectal cancer. Cancer Res. *58*, 248–255.

de Wind, N., Dekker, M., Claij, N., Jansen, L., van Klink, Y., Radman, M., Riggins, G., van der Valk, M., van't Wout, K., and te Riele, H. (1999). HNPCC-like cancer predisposition in mice through simultaneous loss of Msh3 and Msh6 mismatch-repair protein functions. Nat. Genet. *23*, 359–362.

Dignam, J.D., Lebovitz, R.M., and Roeder, R.G. (1983). Accurate transcription initiation by RNA polymerase II in a soluble extract from isolated mammalian nuclei. Nucleic Acids Res. *11*, 1475–1489.

Drummond, J.T., Li, G.M., Longley, M.J., and Modrich, P. (1995). Isolation of an hMSH2-p160 heterodimer that restores DNA mismatch repair to tumor cells. Science *268*, 1909–1912.

Duckett, D.R., Drummond, J.T., Murchie, A.I., Reardon, J.T., Sancar, A., Lilley, D.M., and Modrich, P. (1996). Human MutSalpha recognizes damaged DNA base pairs containing O6-methylguanine, O4-methylthymine, or the cisplatin-d(GpG) adduct. Proc. Natl. Acad. Sci. USA *93*, 6443–6447.

Edelmann, W., Yang, K., Umar, A., Heyer, J., Lau, K., Fan, K., Liedtke, W., Cohen, P.E., Kane, M.F., Lipford, J.R., et al. (1997). Mutation in the mismatch repair gene Msh6 causes cancer susceptibility. Cell *91*, 467–477.

Edelmann, W., Yang, K., Kuraguchi, M., Heyer, J., Lia, M., Kneitz, B., Fan, K., Brown, A.M., Lipkin, M., and Kucherlapati, R. (1999). Tumorigenesis in Mlh1 and Mlh1/Apc1638N mutant mice. Cancer Res. *59*, 1301–1307.

Edelmann, W., Umar, A., Yang, K., Heyer, J., Kucherlapati, M., Lia, M., Kneitz, B., Avdievich, E., Fan, K., Wong, E., et al. (2000). The DNA mismatch repair genes Msh3 and Msh6 cooperate in intestinal tumor suppression. Cancer Res. *60*, 803–807.

Evans, E., and Alani, E. (2000). Roles for mismatch repair factors in regulating genetic recombination. Mol. Cell. Biol. *20*, 7839–7844.

Fink, D., Zheng, H., Nebel, S., Norris, P.S., Aebi, S., Lin, T.P., Nehme, A., Christen, R.D., Haas, M., MacLeod, C.L., and Howell, S.B. (1997). In vitro and in vivo resistance to cisplatin in cells that have lost DNA mismatch repair. Cancer Res. *57*, 1841–1845.

Fishel, R. (2001). The selection for mismatch repair defects in hereditary nonpolyposis colorectal cancer: Revising the mutator hypothesis. Cancer Res. *61*, 7369–7374.

Genschel, J., Littman, S.J., Drummond, J.T., and Modrich, P. (1998). Isolation of MutSbeta from human cells and comparison of the mismatch repair specificities of MutSβ and MutSα. J. Biol. Chem. *273*, 19895–19901.

Gradia, S., Subramanian, D., Wilson, T., Acharya, S., Makhov, A., Griffith, J., and Fishel, R. (1999). hMSH2-hMSH6 forms a hydrolysis-independent sliding clamp on mismatched DNA. Mol. Cell *3*, 255–261.

Guerrette, S., Wilson, T., Gradia, S., and Fishel, R. (1998). Interactions of human hMSH2 with hMSH3 and hMSH2 with hMSH6: Examination of mutations found in hereditary nonpolyposis colorectal cancer. Mol. Cell. Biol. *18*, 6616–6623.

Harfe, B.D., and Jinks-Robertson, S. (2000). DNA mismatch repair and genetic instability. Annu. Rev. Genet. *34*, 359–399.

Heinen, C.D., Schmutte, C., and Fishel, R. (2002). DNA repair and tumorigenesis: Lessons from hereditary cancer syndromes. Cancer Biol. Ther. *1*, 477–485.

Hess, M.T., Gupta, R.D., and Kolodner, R.D. (2002). Dominant Saccharomyces cerevisiae msh6 mutations cause increased mispair binding and decreased dissociation from mispairs by Msh2-Msh6 in the presence of ATP. J. Biol. Chem. *277*, 25545–25553.

Kane, M.F., Loda, M., Gaida, G.M., Lipman, J., Mishra, R., Goldman, H., Jessup, J.M., and Kolodner, R. (1997). Methylation of the hMLH1 promoter correlates with lack of expression of hMLH1 in sporadic colon tumors and mismatch repair-defective human tumor cell lines. Cancer Res. *57*, 808–811.

Karran, P., and Bignami, M. (1994). DNA damage tolerance, mismatch repair and genome instability. Bioessays *16*, 833–839.

Kinzler, K.W., and Vogelstein, B. (1996). Lessons from hereditary colorectal cancer. Cell *87*, 159–170.

Kohler, S.W., Provost, G.S., Fieck, A., Kretz, P.L., Bullock, W.O., Sorge, J.A., Putman, D.L., and Short, J.M. (1991). Spectra of spontaneous and mutagen-induced mutations in the lacI gene in transgenic mice. Proc. Natl. Acad. Sci. USA *88*, 7958–7962.

Koi, M., Umar, A., Chauhan, D.P., Cherian, S.P., Carethers, J.M., Kunkel, T.A., and Boland, C.R. (1994). Human chromosome 3 corrects mismatch repair deficiency and microsatellite instability and reduces N-methyl-N′-nitro-N-nitrosoguanidine tolerance in colon tumor cells with homozygous hMLH1 mutation. Cancer Res. *54*, 4308–4312.

Kolodner, R. (1996). Biochemistry and genetics of eukaryotic mismatch repair. Genes Dev. *10*, 1433–1442.

Kolodner, R.D., and Marsischky, G.T. (1999). Eukaryotic DNA mismatch repair. Curr. Opin. Genet. Dev. *9*, 89–96.

Kolodner, R.D., Tytell, J.D., Schmeits, J.L., Kane, M.F., Gupta, R.D., Weger, J., Wahlberg, S., Fox, E.A., Peel, D., Ziogas, A., et al. (1999). Germ-line msh6 mutations in colorectal cancer families. Cancer Res. *59*, 5068–5074.

Lea, D.E., and Coulson, C.A. (1948). The distribution of the numbers of mutants in bacterial populations. J. Genet. *49*, 246–285.

Li, G.M. (1999). The role of mismatch repair in DNA damage-induced apoptosis. Oncol. Res. *11*, 393–400.

Lin, D.P., Wang, Y., Scherer, S.J., Clark, A.B., Yang, K., Avdievich, E., Jin, B., Werling, U., Parris, T., Kurihara, N., et al. (2004). An Msh2 point mutation uncouples DNA mismatch repair and apoptosis. Cancer Res. *64*, 517–522.

Loeb, L.A. (2001). A mutator phenotype in cancer. Cancer Res. *61*, 3230–3239.

Marsischky, G.T., Filosi, N., Kane, M.F., and Kolodner, R. (1996). Redundancy of Saccharomyces cerevisiae MSH3 and MSH6 in MSH2-dependent mismatch repair. Genes Dev. *10*, 407–420.

Miyaki, M., Konishi, M., Tanaka, K., Kikuchi-Yanoshita, R., Muraoka, M., Yasuno, M., Igari, T., Koike, M., Chiba, M., and Mori, T. (1997). Germline mutation of MSH6 as the cause of hereditary nonpolyposis colorectal cancer. Nat. Genet. *17*, 271–272.

Modrich, P. (1997). Strand-specific mismatch repair in mammalian cells. J. Biol. Chem. *272*, 24727–24730.

Modrich, P., and Lahue, R. (1996). Mismatch repair in replication fidelity, genetic recombination, and cancer biology. Annu. Rev. Biochem. *65*, 101–133.

Myung, K., Datta, A., Chen, C., and Kolodner, R.D. (2001). SGS1, the Saccharomyces cerevisiae homologue of BLM and WRN, suppresses genome instability and homeologous recombination. Nat. Genet. *27*, 113–116.

Nowell, P.C. (1976). The clonal evolution of tumor cell populations. Science *194*, 23–28.

Palombo, F., Gallinari, P., Iaccarino, I., Lettieri, T., Hughes, M., D'Arrigo, A., Truong, O., Hsuan, J.J., and Jiricny, J. (1995). GTBP, a 160-kilodalton protein essential for mismatch-binding activity in human cells. Science *268*, 1912–1914.

Peltomaki, P. (2003). Role of DNA mismatch repair defects in the pathogenesis of human cancer. J. Clin. Oncol. *21*, 1174–1179.

Prolla, T.A., Baker, S.M., Harris, A.C., Tsao, J.L., Yao, X., Bronner, C.E., Zheng, B., Gordon, M., Reneker, J., Arnheim, N., et al. (1998). Tumour

susceptibility and spontaneous mutation in mice deficient in Mlh1, Pms1 and Pms2 DNA mismatch repair. Nat. Genet. *18*, 276–279.

Reitmair, A.H., Redston, M., Cai, J.C., Chuang, T.C., Bjerknes, M., Cheng, H., Hay, K., Gallinger, S., Bapat, B., and Mak, T.W. (1996). Spontaneous intestinal carcinomas and skin neoplasms in Msh2-deficient mice. Cancer Res. *56*, 3842–3849.

Sia, E.A., Kokoska, R.J., Dominska, M., Greenwell, P., and Petes, T.D. (1997). Microsatellite instability in yeast: Dependence on repeat unit size and DNA mismatch repair genes. Mol. Cell. Biol. *17*, 2851–2858.

Thomas, D.C., Umar, A., and Kunkel, T.A. (1995). Measurement of heteroduplex repair in human cell extracts. Methods *7*, 187–197.

Tomlinson, I., and Bodmer, W. (1999). Selection, the mutation rate and cancer: Ensuring that the tail does not wag the dog. Nat. Med. *5*, 11–12.

Umar, A., Koi, M., Risinger, J.I., Glaab, W.E., Tindall, K.R., Kolodner, R.D., Boland, C.R., Barrett, J.C., and Kunkel, T.A. (1997). Correction of hypermutability, N-methyl-N′-nitro-N-nitrosoguanidine resistance, and defective DNA mismatch repair by introducing chromosome 2 into human tumor cells with mutations in MSH2 and MSH6. Cancer Res. *57*, 3949–3955.

Umar, A., Risinger, J.I., Glaab, W.E., Tindall, K.R., Barrett, J.C., and Kunkel, T.A. (1998). Functional overlap in mismatch repair by human MSH3 and MSH6. Genetics *148*, 1637–1646.

Veigl, M.L., Kasturi, L., Olechnowicz, J., Ma, A.H., Lutterbaugh, J.D., Periyasamy, S., Li, G.M., Drummond, J., Modrich, P.L., Sedwick, W.D., and Markowitz, S.D. (1998). Biallelic inactivation of hMLH1 by epigenetic gene silencing, a novel mechanism causing human MSI cancers. Proc. Natl. Acad. Sci. USA *95*, 8698–8702.

Verma, L., Kane, M.F., Brassett, C., Schmeits, J., Evans, D.G., Kolodner, R.D., and Maher, E.R. (1999). Mononucleotide microsatellite instability and germline MSH6 mutation analysis in early onset colorectal cancer. J. Med. Genet. *36*, 678–682.

Wei, K., Clark, A.B., Wong, E., Kane, M.F., Mazur, D.J., Parris, T., Kolas, N.K., Russell, R., Hou, H., Jr., Kneitz, B., et al. (2003). Inactivation of Exonuclease 1 in mice results in DNA mismatch repair defects, increased cancer susceptibility, and male and female sterility. Genes Dev. *17*, 603–614.

Wei, K., Kucherlapati, R., and Edelmann, W. (2002). Mouse models for human DNA mismatch-repair gene defects. Trends Mol. Med. *8*, 346–353.

Wijnen, J., de Leeuw, W., Vasen, H., van der Klift, H., Moller, P., Stormorken, A., Meijers-Heijboer, H., Lindhout, D., Menko, F., Vossen, S., et al. (1999). Familial endometrial cancer in female carriers of MSH6 germline mutations. Nat. Genet. *23*, 142–144.

Wu, Y., Berends, M.J., Mensink, R.G., Kempinga, C., Sijmons, R.H., van Der Zee, A.G., Hollema, H., Kleibeuker, J.H., Buys, C.H., and Hofstra, R.M. (1999). Association of hereditary nonpolyposis colorectal cancer-related tumors displaying low microsatellite instability with MSH6 germline mutations. Am. J. Hum. Genet. *65*, 1291–1298.

Yan, H., Papadopoulos, N., Marra, G., Perrera, C., Jiricny, J., Boland, C.R., Lynch, H.T., Chadwick, R.B., de la Chapelle, A., Berg, K., et al. (2000). Conversion of diploidy to haploidy. Nature *403*, 723–724.

Zhang, H., Richards, B., Wilson, T., Lloyd, M., Cranston, A., Thorburn, A., Fishel, R., and Meuth, M. (1999). Apoptosis induced by overexpression of hMSH2 or hMLH1. Cancer Res. *59*, 3021–3027.